

Full paper

Novel approach to enhance efficiency of hybrid silicon-based solar cells via synergistic effects of polymer and carbon nanotube composite film

Qingxia Fan^{a,b,c}, Qiang Zhang^{a,b}, Wenbin Zhou^{a,b}, Xiaogang Xia^{a,b,c}, Feng Yang^{a,b,c},
Nan Zhang^{a,b}, Shiqi Xiao^{a,b,c}, Kewei Li^{a,b}, Xiaogang Gu^{a,b,c}, Zhuojian Xiao^{a,b,c}, Huiliang Chen^{a,b,c},
Yanchun Wang^{a,b,c}, Huaping Liu^{a,b,c}, Weiya Zhou^{a,b,c,*}, Sishen Xie^{a,b,c,*}

^a Beijing National Laboratory for Condensed Matter Physics, Institute of Physics, Chinese Academy of Sciences, Beijing 100190, China

^b Beijing Key Laboratory for Advanced Functional Materials and Structure Research, Beijing 100190, China

^c University of Chinese Academy of Sciences, Beijing 100049, China

ARTICLE INFO

Keywords:

Carbon nanotubes
Carbon nanotube composite film
Hybrid silicon solar cells

ABSTRACT

In this work, we put forward an effective approach by combining both highly transparent and conductive carbon nanotube (CNT) network and poly (3, 4-ethylene dioxythiophene):poly (styrenesulfonate) (PEDOT:PSS) film to co-form-coordinate heterojunctions with silicon, and have developed a hybrid PEDOT:PSS-CNT/n-Si solar cell. The power conversion efficiency (PCE) of the as-designed solar cell can be improved up to 10.2%, which is much higher than the PCE values of both PEDOT:PSS/n-Si (5.5%) and CNT/n-Si (6.1%) solar cells fabricated using the same materials and process. PEDOT:PSS can fill the hundreds nanometer scale pores of the CNT network, both CNT network and PEDOT:PSS patches contact with the silicon concomitantly and form $p_{\text{Synergy}}-n$ heterojunctions through seamless contact with n-Si. The PEDOT:PSS-CNT composite film exhibits a much lower sheet resistance and remains high optical transmittance. Once the photo-generated holes are extracted to the PEDOT:PSS-CNT composite film, CNT network can serve as a carrier transport bridge, which is different from the design that inserts an ultrathin polymer between the CNT and Si. Incorporation of the continuous CNT network with PEDOT:PSS jointly in the as-designed simple and explicit structure has generated synergistic effects, which can make full use of the respective merits and then considerably enhance the PCE of hybrid PEDOT:PSS-CNT/n-Si solar cells.

1. Introduction

Over the past decades, there has been an enormous interest in developing photovoltaic devices using carbon nanotube (CNT), since CNTs can form a two-dimensional network exhibiting outstanding optical and electrical properties [1]. CNT has high carrier mobility ($\sim 10^5 \text{ cm}^2 \text{ V}^{-1} \text{ s}^{-1}$) [2], high current carrying capacity ($> 10^9 \text{ A cm}^{-2}$) [3,4], and tunable band gap. On the other hand, traditional silicon solar cells still dominate the photovoltaic market at present because of its superior stability and high power conversion efficiency (highest record is 25.6%), while they suffer rigorous ion implantation, annealing processes and doping at high temperature [5]. In order to avoid these complicated process, therefore, hybrid CNTs and silicon heterojunction solar cells have been extensively studied that take advantages of superior optoelectronic properties of CNT and mature silicon technologies [6–11], especially since the heterojunction between p-CNT and n-Si can form at room temperature. In the past few years, about 12%

efficiency has been achieved by optimized the optical transmittance of CNT films for small area (window size of 1 mm in diameter) CNT/Si solar cell [9]. Some researchers improved the photovoltaic performance by means of post-processing, for example, infiltrating nitric acid into the heterojunction [12], coating CNT film surface with metal oxide layers such as TiO_2 [13,14] and MoO_x [15]. Since the ionic liquid electrolyte between the CNT networks and Si could electrically modulate the Fermi level offset and the junction interface dipole, the power conversion efficiency of as-prepared device could reach 8.4% and be adjusted between 4% and 11% continuously and reversibly [8]. It was revealed that dominant photocarriers are generated in Si and then the carriers transport mechanism is diffusion-dominated p-n junction transport [7]. There are also some researches about influence of the CNTs' conductivity type and chirality on the CNT/Si solar cells [11,16,17].

Heterojunction solar cells based on p-type conjugated polymers and n-Si is another alternative to the traditional silicon solar cells, which

* Corresponding authors at: Beijing National Laboratory for Condensed Matter Physics, Institute of Physics, Chinese Academy of Sciences, Beijing 100190, China.
E-mail addresses: wyzhou@iphy.ac.cn (W. Zhou), ssxie@iphy.ac.cn (S. Xie).

could be made through solution processing at mild temperature [18–22]. The most commonly used conductive polymer, poly (3, 4-ethylene dioxathiophene): poly (styrenesulfonate) (PEDOT:PSS), which is well known as a hole transport layer in organic solar cells, exhibits fairly high conductivity and transparency. In recent years, a variety of investigations have been carried out on hybrid polymer/n-Si solar cells [23–26], including various interface engineering and surface modification to improve the performance of devices reported widely [27–32]. The excellent efficiency values of 11% and 14.14% are obtained by combination of heavy doping, anisotropy etching in Si wafers (e.g., nanocones or bowl-like nanopores), provided excellent antireflection function, and forming a strong inversion layer and a hole block layer by inserting a layer of 1, 4, 5, 8, 9, 11-hexaazatriphenylene hexacarbonitrile and a nanoscale perylene diimide layer, respectively [31–33]. However, if n-Si, without decoration, is used in the hybrid PEDOT:PSS/n-Si solar cells, the efficiency are between 1.6–10.26% [33–37].

Several researchers report about improving efficiency of hybrid solar cells by dispersion of CNTs into PEDOT:PSS [34], this approach is inadequate mainly because the CNTs are randomly dispersed in the conductive polymer, so the efficiency enhancement (e.g., from 10.26% to 10.93%) by incorporating the CNTs is quite limited. In the literature, since CNTs are very short (about several micrometers), they contact by X-type junctions that formed under room temperature. Because of the weak interaction between short CNTs contacted by X-type junctions, PEDOT:PSS could open the X-type junction. Therefore, the continuous CNT conductive path cannot be constituted. Inserting a polymer between the silicon and CNTs [38,39], in which the thickness of the polymer must be controlled carefully to 10 nm, can also promote the efficiency (from 6.0% of Si-CNT to 7.7% of Si-PEDOT:PSS-CNT) by creating a better depletion layer within silicon. In these structures mentioned above, since a lot of short CNTs were randomly dispersed in the conductive polymer or coated on polymer, CNTs did not directly participate in the formation of heterojunctions with silicon. The excellent optical and electrical properties of CNTs were not fully utilized in these assemblies of hybrid silicon solar cells. Our CNT continuous network was directly synthesized by CVD, in which the CNT bundles are interconnected well with each other by Y-type junctions [40,41] that formed at high-temperature synthesis process, as shown in Fig. S1 and Fig. 2b. And individual CNT is super long, larger than several hundred micrometers. What's more, because of the strong interaction between CNT bundles interconnected by Y-type junctions, PEDOT:PSS could not open the Y-type junction, there is a continuous conductive path formed in CNT network. Besides, what if both the CNTs and conductive polymer participate in the formation of heterojunction with Si?

In the present work, we put forward a novel approach by combining both highly transparent and conductive CNT network and PEDOT:PSS film to co-form-coordinate heterojunctions with silicon through seamless contact of entire area for efficient carriers separation and transport, and have developed a hybrid PEDOT:PSS-CNT/n-Si solar cell in which both CNT network and PEDOT:PSS can take their advantages synergistically. The efficiency of the as-designed solar cell can be improved up to 10.2%. The outstanding performance of the as-designed hybrid solar cell verifies the validity of this approach, which opens up a promising way to a highly efficient, highly reproducible and highly scalable preparation of photovoltaic devices.

2. Experimental section

2.1. Synthesis of CNT films

The large area and freestanding CNT films with high optical transmittance and low sheet resistance were prepared by a developed chemical vapor deposition method. In brief, methane and ferrocene with a small quantity of sulfur were used as carbon source and catalyst

precursor, respectively. The catalyst precursor sublimated at ~ 100 °C and methane (~ 10 sccm) mixed with Ar served as carrier gas arrived at the reaction furnace. The growth temperature was set at 1050 °C and the growth time was controlled between several minutes and hours. The transmittance and thickness of the as-synthesized CNT film could be controlled by adjusting the growth parameters, such as growth time and carbon feedstock etc. The CNT film was immersed in Nitric acid (65 wt%) for 5 h to remove the residual catalysts and then washed with deionized water repeatedly before used.

2.2. Solar cell devices fabrication

A 500 nm thermal oxide SiO₂ covered and one side polished n-type Si (100) wafer with bulk resistivity 1–5 Ω cm was patterned with square windows (3 \times 3 mm²) by ultraviolet photolithography. The thermal oxide SiO₂ was etched by the BOE solution (volume ratio of NH₄F (40 wt% aqueous solution) and HF (40 wt%) is 6:1). Before the solar cell's fabrication, the patterned Si substrate was treated with 0.5 M nitric acid for one minute, so the Si surface was coated with an ultrathin silicon oxide. The silicon oxide in our solar cell may be a little thicker for the PEDOT:PSS/n-Si solar cell, which treated with 10% nitric acid for 3 s is best [42]. The thin oxide layer on Si surface can help to suppress the charge recombination and increase the minority carrier lifetime [43,44]. For PEDOT:PSS/n-Si solar cells, the PEDOT:PSS solution (Clevios PH 1000, purchased from Heraeus) was prepared by mixing 5 vol% dimethylsulfoxide (DMSO) and 1 vol % Zonyl FS-300 fluorosurfactant (obtained from Alfa Aesar). PEDOT:PSS solution was spun coated on the patterned silicon substrates at different spin speeds (2000, 3000 and 4000 rpm) and then annealed at 120 °C for 15 min in the air. For CNT/n-Si solar cells, a piece of CNT film was firstly mounted onto a PET frame with desired square hole, then a few drops of ethanol on the PET frame can help the CNT film tightly adhere to the PET frame when the ethanol is evaporated. When preparing the CNT/n-Si solar cell, the CNT film at the central hole of the PET frame was transferred onto the surface of Si. A drop of ethanol is indispensable to ensure a tight contact between CNT film and silicon as well. We use blade to cut the CNT film, and take away PET frame. Therefore, there is no PET on a completed device. For the composite PEDOT:PSS-CNT/n-Si solar cells, we put the CNT network on the silicon first, and after fully volatilization of ethanol, the PEDOT:PSS solution was spun coated on the CNT network. More than ten devices were prepared at each spin speed. The anode was made by painting the silver paste around the active window, and Eutectic Gallium-Indium (EGaIn, obtained from Alfa Aesar) was applied to the back side of Si, which served as cathode. The stability of CNT/n-Si solar cells in air is quite well within one week. However, because the PEDOT:PSS is strongly hygroscopic [45,46], its resistance increase gradually. The stability of PEDOT:PSS-CNT/n-Si solar cells in air is poor, the PCE drops to about 78% of the original PCE within one day in air.

2.3. Characterization and measurements

The optical transmission spectra of CNT network, PEDOT:PSS and PEDOT:PSS-CNT composite film were measured utilizing a UV-Vis-NIR spectrophotometer (UV-3600, Shimadzu). The performances of the solar cells were carried out using a solar simulator (CHF-XM 500, Beijing Trusttech Co. Ltd.) under AM 1.5 G with a calibrated irradiation intensity of 100 mW/cm². The outer area except the active window was covered with an opaque mask to shield the incident light. The J-V data were collected using a Keithley 4200-SCS. Raman spectra were recorded using LabRAM HR 800 (HORIBA Jobin Yvon Inc.). The morphology of the CNT network and PEDOT:PSS-CNT composite film was characterized by SEM (Hitachi S-5200) and AFM (Bruker MultiMode-8 ScanAsyst). We scratched the composite PEDOT:PSS-CNT film and made the composite film at the edge of the scratch turn

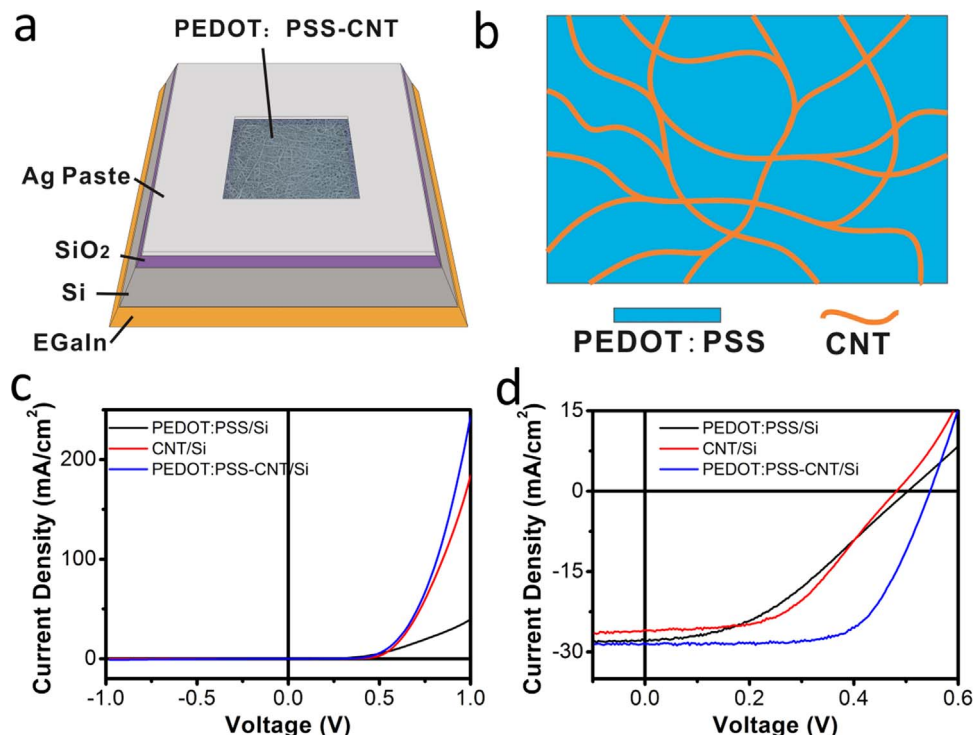


Fig. 1. (a) Schematic of the PEDOT:PSS-CNT/n-Si solar cell. (b) Diagram of the back surface of the PEDOT:PSS-CNT composite film at the interface between it and n-Si. J-V characteristics of PEDOT:PSS/n-Si, CNT/n-Si and PEDOT:PSS-CNT/n-Si heterojunction solar cells: (c) in the dark and (d) under illumination of a simulated AM 1.5 G 100 mW/cm² solar light. CNT network with an optical transmittance of about 75% was used and PEDOT:PSS solution was spin-coated at 3000 rpm.

over, in order to observe the back surface morphology. Sheet resistances of the three types of films were measured by Keithley 2400 with a four-electrode method. We determined the thickness of the films from the Bruker Dektak XT stylus profiler. The work functions of the different films were measured by an ultraviolet photoemission spectroscopy (UPS) on Thermo Scientific ESCALab 250Xi instruments.

3. Results and discussion

Fig. 1a shows the schematic of the as-designed device structure of a hybrid PEDOT:PSS-CNT/n-Si heterojunction solar cell. An ultrathin freestanding CNT network exhibits a continuously porous spider web like structure, shown in Figs. 2a and 2b, in which the CNT bundles interconnected well with each other by Y-type junction. Such a structure enables the CNT network to possess high electrical and mechanical properties. It was transferred to the pre-patterned n-Si/SiO₂ wafer, where the thermal oxidation SiO₂ was etched using a buffered oxide etch (BOE) solution and the exposed n-Si was regarded as active window. The square active window where the Si was exposed was defined as the active area of the solar cell. The flexibility of the CNT network makes it compliant with the active window and contact tightly to the exposed n-Si, forming heterojunctions conformally at the interface between the CNT bundles and silicon. Nevertheless, the effective heterojunction area, i.e., the contacting portion between the CNT bundles and Si, accounts for less than 35% of the area of silicon active window (obtained from the atomic force microscope images of CNT network) because the porosity of as-used CNT network is rather high. Then, PEDOT:PSS solution was spin-coated on the CNT/n-Si at different spin speed followed by thermal annealing. With spin coating a layer of about 90–140 nm thick PEDOT:PSS, the surface of the hybrid film becomes flat, and the CNT spider network structure cannot be observed from the top of PEDOT:PSS-CNT composite film, as shown in Figs. 2c and d. In Figs. 2e and f, it is clearly observed that PEDOT:PSS can patch the hundreds nanometer scale pores of the CNT network. So, both the CNTs or their bundles and the PEDOT:PSS

patches filling the voids of CNT network contact with the silicon concomitantly and increase the effective p-n junction area. The back surface structure of PEDOT:PSS-CNT composite film is schematically illustrated in Fig. 1b and figuratively conjures up a “highway network”, i.e., spider network of CNTs or CNT bundles act like the interconnected “highways” crisscrossing the “continent” made of PEDOT:PSS film.

In order to understand the mechanism of the as-designed solar cells, we also fabricated a basic CNT/n-Si solar cell and a PEDOT:PSS/n-Si solar cell without any additional processing (top grid lines, elaborately decoration of Si or combination of a strong inversion layer and a nanoscale hole block layer *etc.*), where only a CNT network or a PEDOT:PSS film coated on silicon, respectively.

The current density-voltage (J-V) characteristics of the three types of hybrid solar cells: PEDOT:PSS-CNT/n-Si, PEDOT:PSS/n-Si, and CNT/n-Si were measured in the dark (Fig. 1c) and under illumination with a simulated air mass (AM) 1.5 G 100 mW/cm² solar light (Fig. 1d). The J-V characteristics measured in the dark (Fig. 1c) clearly reveals the diode properties for all of the three types of solar cells. The composite PEDOT:PSS-CNT/n-Si solar cell exhibits much higher rectification ratio than the other two solar cells. Fig. 1d shows all devices display typical photovoltaic behavior. In general, solar cell incorporated with PEDOT:PSS-CNT composite film and Si shows more desirable J-V characteristics than those incorporated with only PEDOT:PSS film or CNT network. The PEDOT:PSS-CNT/n-Si solar cell exhibits a better performance: a short-circuit current density (J_{sc}) of 28.6 mA/cm², an open-circuit voltage (V_{oc}) of 548 mV, a fill factor (FF) of 65.4% and a high power conversion efficiency (PCE) of 10.2%, whereas for the PEDOT:PSS/n-Si solar cell and the CNT/n-Si solar cell the J_{sc} are 27.8 and 25.9 mA/cm², V_{oc} are 502 and 481 mV, FF are 39.2% and 49.0%, and PCE are 5.5% and 6.1%, respectively (Fig. 1d). Excitingly, the efficiency of composite PEDOT:PSS-CNT/n-Si solar cell was improved by about 67% in comparison to the CNT/n-Si solar cell, and the enhancement can be primarily attributed to the improvement of FF, which is enhanced by about 33%. When compared with PEDOT:PSS/n-Si solar cell, the as-designed device shows 85% im-

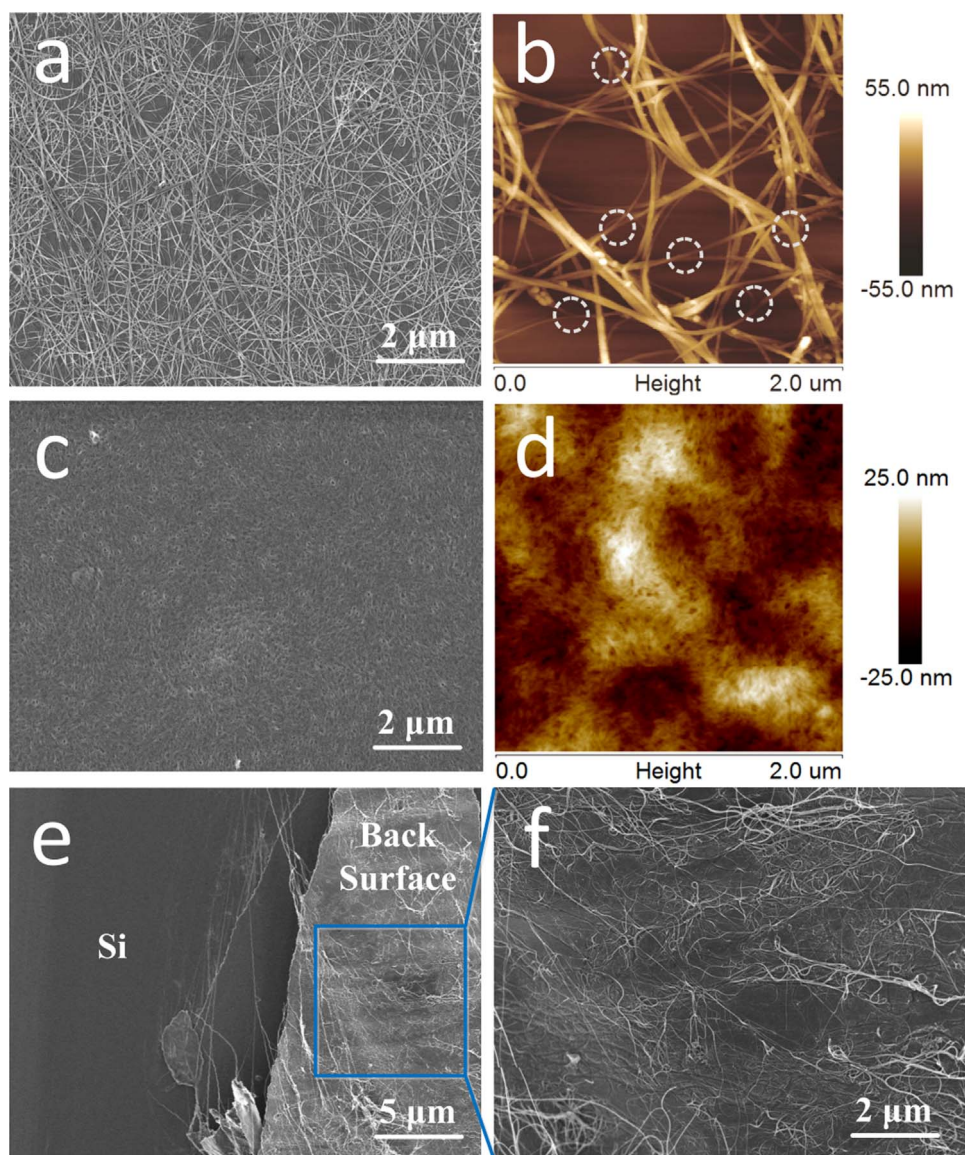


Fig. 2. Scanning electron microscope (SEM) and atomic force microscope (AFM) images of (a, b) CNT network, white circles in (b) show the Y-type junctions in CNT network; (c, d) front surface of PEDOT:PSS-CNT composite film. SEM images of (e) interface between the PEDOT:PSS-CNT composite film and silicon, (f) back surface of PEDOT:PSS-CNT composite film.

provement in efficiency and over 67% enhancement in FF. It can be suggested that the as-designed solar cell incorporated with hybrid PEDOT:PSS-CNT film more effectively suppresses the carriers recombination and promotes the carriers extraction. So, why has the PCE of as-designed hybrid PEDOT:PSS-CNT/n-Si solar cell been improved so significantly, even nearly reached the sum of the PCE values of both PEDOT:PSS/n-Si and CNT/n-Si solar cells?

Since CNT network or PEDOT:PSS film act as a transparent and conductive film for light passing through, carriers separation and transportation, its optical transparency and conductivity should significantly influence the performance of the solar cells. For our CNT film with spider like network structure, the thinner and sparse CNT network has a higher optical transmittance that can ensure more photons reaching the Si substrate and producing more photo-generated carriers. On the other hand, thicker and dense CNT network shows lower sheet resistance that can enhance the ability of transporting photo-generated carriers, and the high surface density can also increase the effective area of p-n junctions. Therefore, there is a tradeoff between the optical transmittance and sheet resistance of the CNT network. Similarly, PEDOT:PSS deposited at various spin speed manifest that

different optical transmittance and sheet resistance will strongly influence the performance of the solar cells. We also carried out systematic experiments on CNT networks with different optical transmittance and PEDOT:PSS films with various thicknesses. Detailed results are summarized in Table 1 and Fig. S2. It can be revealed from the measured photovoltaic parameters (Table 1) that all the devices incorporated with PEDOT:PSS-CNT composite films exhibit improved efficiencies in comparison to those with only CNT networks or PEDOT:PSS films. The spin coating speed for the PEDOT:PSS is optimized at 3000 rpm in the situation that CNT network with 75% optical transmittance was incorporated (Fig. S3). Different from that of the PEDOT:PSS-CNT/n-Si solar cells, the optimal spin speed for the PEDOT:PSS/n-Si is 2000 rpm, because the optical transmittance and conductivity of the two films are quite different. The performance data of the PEDOT:PSS-CNT/n-Si solar cells incorporating CNT networks with optical transmittance of ~80% (relatively thin) and ~70% (relatively thick) are summarized in the Fig. S4, Fig. S5, Table S2 and Table S3.

The reflectance spectra of the PEDOT:PSS/n-Si, CNT/n-Si and PEDOT:PSS-CNT/n-Si solar cells (Fig. 3a) are recorded to evaluate the

Table 1

Photovoltaic properties of the PEDOT:PSS/n-Si, CNT/n-Si and PEDOT:PSS-CNT/n-Si solar cells. The optical transmittance of the used CNT networks is about 75%.

Device	Spin coating speed [rpm]	Thickness [nm]	J_{sc} [mA/cm^2]	V_{oc} [mV]	FF [%]	PCE [%]	R_s [$\Omega\text{-cm}^2$]	n
PEDOT:PSS /Si	2000	138	24.9	558	49.1	6.8	6.6	4.4
CNT/Si	–	72	26.6	495	51.1	6.7	1.7	3.4
PEDOT:PSS-CNT/Si	2000	224	29.0	541	61.2	9.6	1.6	3.4
PEDOT:PSS /Si	3000	118	27.8	502	39.2	5.5	6.7	5.9
CNT/Si	–	72	25.9	481	49.0	6.1	1.5	3.9
PEDOT:PSS-CNT/Si	3000	171	28.6	548	65.4	10.2	1.2	3.8
PEDOT:PSS /Si	4000	91	25.3	523	41.6	5.5	8.1	5.3
CNT/Si	–	72	27.4	485	51.6	6.9	1.8	3.3
PEDOT:PSS-CNT/Si	4000	153	26.8	548	62.6	9.2	1.7	4.1

antireflection effect of the PEDOT:PSS film. A polished Si without textures exhibits about 37% reflectance between 400 nm and 1100 nm. The reflectivity of the CNT/n-Si solar cell is slightly lower than that of the bare Si, about 28% across the visible region because of the optical absorption of CNT film. However, the PEDOT:PSS/n-Si solar cell shows a relatively low reflectance (average 10%) between 600 nm and 900 nm where the silicon can absorb maximum solar radiation. The wavelength corresponding to the minimum reflectance shows a red shift for the PEDOT:PSS-CNT/n-Si compared to PEDOT:PSS/n-Si, because the thickness of PEDOT:PSS-CNT composite film increases when incorporating the CNT network as shown in Fig. 3c. In order to guarantee a as low as possible reflectance in the visible region, the thickness of the hybrid PEDOT:PSS-CNT film should be appropriate. When the spin speed of the PEDOT:PSS is 3000 rpm, the reflectance is lower in the visible region as shown in Fig. S6. The reflectance of the PEDOT:PSS-CNT/n-Si is much lower than the other two devices in entire wavelength, which could give rise to more photo-generated carriers due to the increase in light absorption by silicon. Therefore, the enhancement of J_{sc} should be partially ascribed to the antireflection effect of CNT and PEDOT:PSS. It is very exciting that the PEDOT:PSS serves as not only the p-type conductive polymer which fill the pores in

a CNT network to form p-n heterojunction with the Si, but also the antireflection layer to ensure that the solar cells can absorb more sunlight.

The optical transmittance spectra and sheet resistance of the CNT networks, PEDOT:PSS films and hybrid PEDOT:PSS-CNT films are shown in Fig. 3b. The as-synthesized CNT networks have both low sheet resistance and high optical transmittance, which are much superior to those fabricated by filtrating suspended CNTs solution [47]. PEDOT:PSS film also shows extremely high transmittance above 90% (Fig. S7). Thus the optical transmittance decreases slightly from 82% of the CNT network to 78% of the composite film (PEDOT:PSS spin coated at 3000 rpm). This drop could be compensated by the antireflection effect of the PEDOT:PSS film to an extent. As a consequence, the J_{sc} of the PEDOT:PSS-CNT/n-Si solar cells remains almost the same with that of the CNT/n-Si solar cells (Table 1 and Table S1).

In our solar cells without top grid line electrode, the sheet resistance of the top thin film contributes a majority of series resistance of the solar cells, since the holes need to travel through the thin film, get to the external electrode and then be collected. Spin coating PEDOT:PSS on the CNT network leads to an enormous reduction of

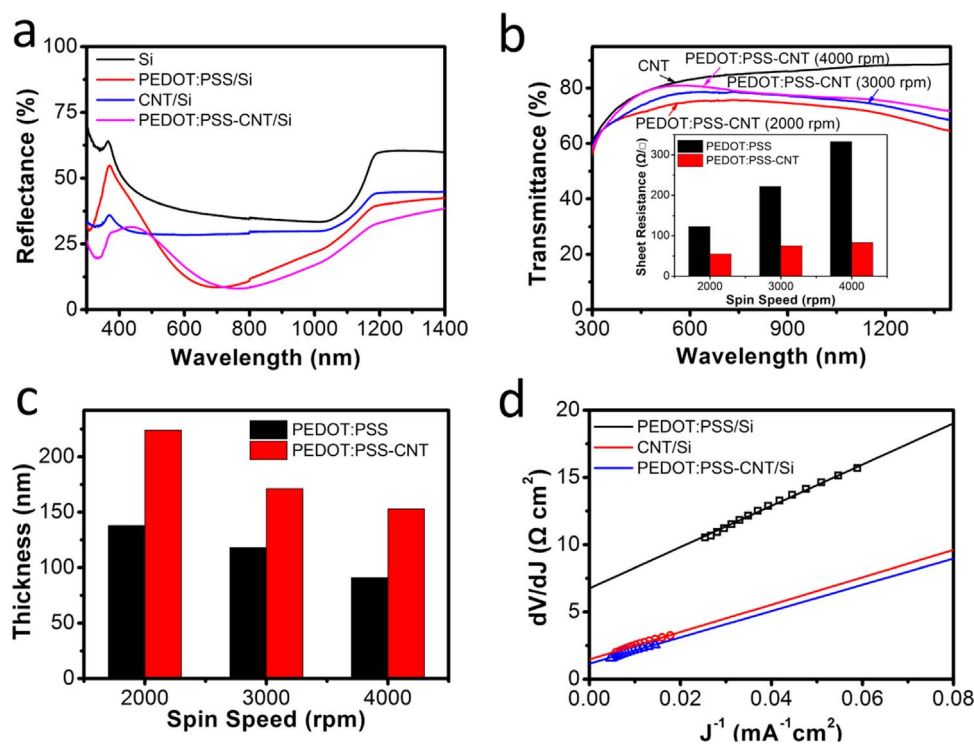


Fig. 3. (a) Reflectance spectra of a Si, PEDOT:PSS/n-Si, CNT/n-Si and PEDOT:PSS-CNT/n-Si solar cell. (b) Optical transmittance spectra of CNT film and PEDOT:PSS-CNT composite films. The inset shows the sheet resistance of the PEDOT:PSS and PEDOT:PSS-CNT composite films. (c) Thickness vs spin speed of PEDOT:PSS and PEDOT:PSS-CNT films. The CNT films with transmittance of 82% were used. (d) dV/dJ as a function of J^{-1} for PEDOT:PSS/n-Si, CNT/n-Si and PEDOT:PSS-CNT/n-Si heterojunction solar cells, the spin coating speed of PEDOT:PSS was 3000 rpm, and the CNT film with transmittance of 75% was used.

the sheet resistance, which dropped from 222 Ω/\square for PEDOT:PSS (at the 3000 rpm spin speed) and 135 Ω/\square for the hybrid PEDOT:PSS-CNT films. The phenomena are also reflected in Fig. 1c. It can be concluded that the conductivity could be improved substantially while the transmittance reduced slightly by combining the PEDOT:PSS and CNT network together.

To further clarify the photovoltaic characteristics of the solar cells, the series resistance (R_s) and the diode ideality factor (n) were determined as shown in Fig. 3d and Table 1. According to the equivalent circuit model, the J-V characteristics can be described as [48].

$$J=J_0 \left[\exp \left(\frac{e(V-R_s J)}{nk_B T} \right) - 1 \right] + \frac{V-R_s J}{R_{sh}} - J_{ph} \quad (1)$$

where J_0 is the reverse saturated current density, e is the electron charge, k_B is the Boltzmann constant, T is the absolute temperature, R_{sh} is the shunt resistance, and J_{ph} is the light induced current density. It can be deduced that (when R_{sh} is very large)

$$\frac{dV}{dJ} = \frac{nk_B T}{e} (J + J_{ph})^{-1} + R_s \quad (2)$$

In the dark measurements, a linear fitting curve of dV/dJ versus J^{-1} gives the specific values of n from the slop and R_s from the intercept.

Based on the above analysis and discussion of the experimental results for as-designed hybrid PEDOT:PSS-CNT/n-Si solar cells, we find that to improve the fabrication parameters, such as optimized optoelectronic properties, optimal antireflection layer, and increase contact area of p-type layer with n-Si, are imperative and directly beneficial for the device's performance, but not enough to result in such a big and primary effect revealed in Fig. 1d and Table 1. So, what is the root cause of the marked increase in the efficiency of our designed PEDOT:PSS-CNT/n-Si solar cells?

The heterojunction solar cell presented here typically consists of a n-type monocrystalline silicon substrate coated with a thin p-type layer, such as CNTs, conductive polymer, or their composites. Our CNT network is dominant p-type in atmosphere [49], and we also immerse it into the nitric acid for further p-doping [50]. As for the PEDOT:PSS/n-Si solar cells, the junction has been described as a p-n junction by varying the n-Si doping concentrations [19,51]. As shown in Fig. S8 and Fig. 4a, the work functions (ϕ) of CNT network, PEDOT:PSS film, and PEDOT:PSS-CNT composite film measured by ultraviolet photoemission spectroscopy (UPS) were 4.82 eV, 5.44 eV and 5.0 eV, respectively. The energy band gap of silicon is 1.12 eV and the Fermi level is 4.25 eV for the doping concentration of 10^{16} cm^{-3} [52]. Thus, in the PEDOT:PSS-CNT/n-Si solar cell, beyond the p-n heterojunctions formed by PEDOT:PSS patches and CNT bundles with silicon substrate individually, their corporate effect is more important. As shown in Fig. 4b, the Fermi level offset between the PEDOT:PSS-CNT composite film and n-Si produces a built-in voltage (V_{bi}) of about 0.75 V, which is larger than that of a CNT network (0.57 V). The mechanism of the as-designed hybrid solar cell is schematically shown in Fig. 4c. Photons transmitted through the transparent PEDOT:PSS-CNT composite film and were absorbed by the Si, generating electron-hole pairs that are separated by the built-in voltage at the interface, where the holes were extracted to the p-type layer and the electrons to the n-Si side, and finally the holes and electrons were collected by external electrodes, respectively. It is worth mentioning that the holes in the PEDOT:PSS patches can also transfer to the interconnected CNT network because of the mutually doping between PEDOT:PSS and CNT network, the corporate effect of both contact with n-Si form another kind p-n junction, $p_{\text{Synergy-n}}$. Although the conductive polymer film shows poor mobility which severely limits the hole transport [53], continuous CNT network can serve as a carrier transport bridge like "highways" because the CNTs have high carrier (both electron and hole) mobility along

their one-dimensional axis [54,55]. Once the photo-generated holes were extracted under the larger built-in voltage to the PEDOT:PSS-CNT composite film, they can be transported quickly to the external circuit through the interconnected CNT "highways". Therefore, in our designed hybrid solar cell, the unique approach can not only play an excellent conductive role of CNTs, but also use PEDOT:PSS to increase the effective area of p-n junction, and in particular generate synergistic effects of $p_{\text{Synergy-n}}$ to substantially promote the solar cell's PCE.

In brief, the effective enhancement in the performance for the PEDOT:PSS-CNT/n-Si solar cell can be attributed to the synergistic effects of PEDOT:PSS patches and continuous CNT network. First, the PEDOT:PSS-CNT composite film exhibits a much lower sheet resistance, while the optical transmittance is still maintained (Fig. 3b). Second, the PEDOT:PSS-CNT composite film forms a seamless contact with n-Si at entire active area as shown in Fig. 4c, which markedly increases the effective heterojunction area and improves the FF of as-designed hybrid solar cell. Third, carriers in the PEDOT:PSS patches can transfer to the interconnected CNT network. So, incorporating CNT network can promote the hole transport ability of PEDOT:PSS. Overall, incorporation of the continuous CNT network with PEDOT:PSS jointly in the as-designed simple and explicit structure has generated the marked synergistic effects, which can not only make full use of the respective merits but also considerably reduce the R_s and n , greatly enhance the PCE and the FF of hybrid PEDOT:PSS-CNT/n-Si solar cells. This co-form-coordinate heterojunctions with silicon structure is quite different from inserting a polymer between the CNTs and Si [39]. As for mechanism, in our solar cells, both CNT and PEDOT:PSS can contact with Si and form heterojunctions, while in previous works [34,39], CNTs cannot contact with silicon and do not directly participate in the formation of heterojunctions. Furthermore, the as-synthesized CNT continuous network is used as a carrier transport bridge like "highways", in which the CNT bundles interconnected well with each other by Y-type junction [40,41]. Randomly dispersed CNTs used in literature [7,17,39], in which the short CNTs connected with each other by X-type junction. For the reasons given above, we have got a higher efficiency. The role of the CNTs and conductive polymer in the hybrid solar cells have also illustrated through a basic and deliberate structure design.

4. Conclusions

In conclusion, we have developed an effective approach to improve efficiency of a hybrid PEDOT:PSS-CNT/n-Si solar cell with a simple and explicit structure, in which the hundreds nanometer scale pores of the CNT network can be filled by PEDOT:PSS patches. Both the PEDOT:PSS patches and CNT "highway network" can co-form-coordinate heterojunctions with the silicon substrate and fully contribute their advantages. We exploited their synergistic effects and greatly improved the photovoltaic performances of the hybrid PEDOT:PSS-CNT/n-Si solar cells, based on analysis of the three types of basic solar cells fabricated under the same preparation condition, employing silicon without any nanostructure. By optimized the experimental parameters of incorporation of PEDOT:PSS and CNT network, the power conversion efficiency of the as-designed hybrid solar cell is 10.2%, which has been enhanced about 67% and 85% in comparison to the CNT/n-Si (6.1%) and PEDOT:PSS/n-Si (5.5%) solar cell fabricated using the same materials and process, respectively. Our findings also put forward a new way for manufacturing highly efficient, highly reproducible and easily scaling-up hybrid polymer-CNT film based photovoltaic devices.

Acknowledgements

This work was supported by the National Basic Research Program of China (Grant No. 2012CB932302), the National Natural Science Foundation of China (11634014, 51172271, 51372269 and

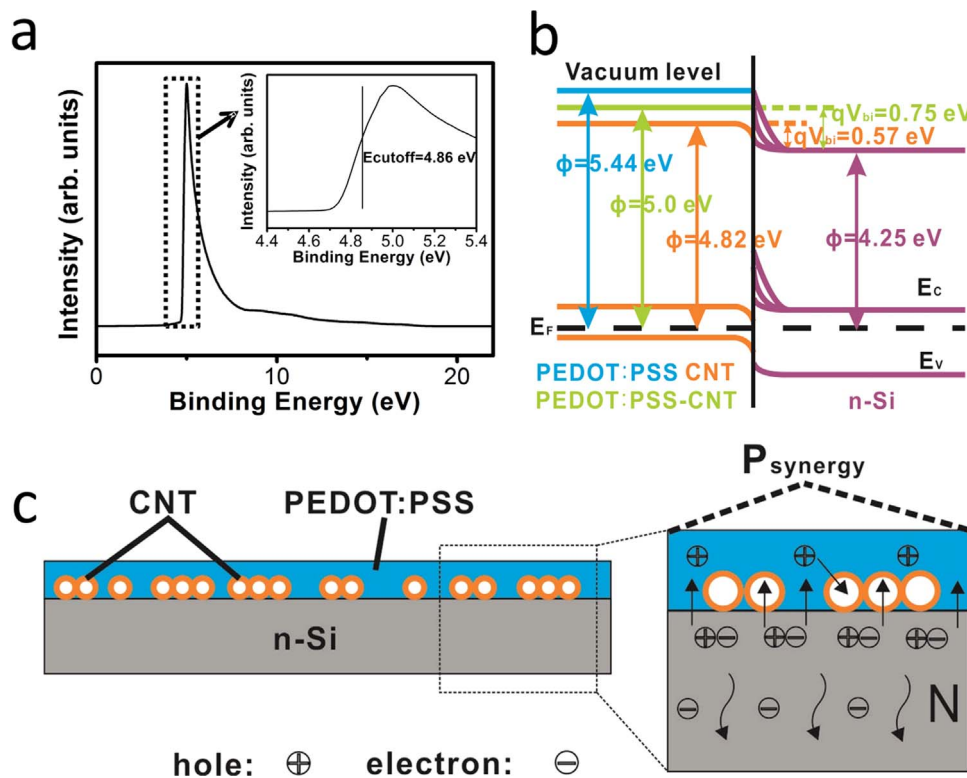


Fig. 4. (a) UPS spectrum of PEDOT:PSS-CNT composite film. The work function of PEDOT:PSS-CNT composite film is 5.0 eV, which is calculated through the equation: $h\nu - \phi = E_{\text{Fermi}} - E_{\text{cutoff}}$, where $h\nu = 21.22$ eV, $E_{\text{Fermi}} = 21.08$ eV, E_{cutoff} is the mid-point of the cutoff line. (b) Energy band diagram of the fabricated devices. (c) Schematic of the mechanism of as-designed hybrid PEDOT:PSS-CNT/n-Si solar cell.

51472264), the “Strategic Priority Research Program” of the Chinese Academy of Sciences (XDA09040202). Dr. H. P. Liu thanks support by the Recruitment Program of Global Youth Experts and the “100 talents project” of CAS.

Appendix A. Supplementary material

Supplementary material associated with this article can be found in the online version at <http://dx.doi.org/10.1016/j.nanoen.2017.02.003>.

References

- [1] R.C. Tenent, T.M. Barnes, J.D. Bergeson, A.J. Ferguson, B. To, L.M. Gedvilas, M.J. Heben, J.L. Blackburn, *Adv. Mater.* 21 (2009) 3210–3216.
- [2] T. Durkop, S.A. Getty, E. Cobas, M.S. Fuhrer, *Nano Lett.* 4 (2004) 35–39.
- [3] A. Javey, J. Guo, Q. Wang, M. Lundstrom, H.J. Dai, *Nature* 424 (2003) 654–657.
- [4] Z. Yao, C.L. Kane, C. Dekker, *Phys. Rev. Lett.* 84 (2000) 2941–2944.
- [5] M.A. Green, K. Emery, Y. Hishikawa, W. Warta, E.D. Dunlop, *Prog. Photovolt.* 23 (2015) 805–812.
- [6] Y. Jia, J. Wei, K. Wang, A. Cao, Q. Shu, X. Gui, Y. Zhu, D. Zhuang, G. Zhang, B. Ma, L. Wang, W. Liu, Z. Wang, J. Luo, D. Wu, *Adv. Mater.* 20 (2008) 4594–4598.
- [7] Y. Jung, X.K. Li, N.K. Rajan, A.D. Taylor, M.A. Reed, *Nano Lett.* 13 (2013) 95–99.
- [8] P. Wadhwa, B. Liu, M.A. McCarthy, Z.C. Wu, A.G. Rinzler, *Nano Lett.* 10 (2010) 5001–5005.
- [9] F. Wang, D. Kozawa, Y. Miyauchi, K. Hiraoka, S. Mouri, Y. Ohno, K. Matsuda, *ACS Photonics* 1 (2014) 360–364.
- [10] K. Cui, A.S. Anisimov, T. Chiba, S. Fujii, H. Kataura, A.G. Nasibulin, S. Chiashi, E.I. Kauppinen, S. Maruyama, *J. Mater. Chem. A* 2 (2014) 11311–11318.
- [11] J.M. Harris, R.J. Headrick, M.R. Semler, J.A. Fagan, M. Pasquali, E.K. Hobbie, *Nanoscale* 8 (2016) 7969–7977.
- [12] Y. Jia, A.Y. Cao, X. Bai, Z. Li, L.H. Zhang, N. Guo, J.Q. Wei, K.L. Wang, H.W. Zhu, D.H. Wu, P.M. Ajayan, *Nano Lett.* 11 (2011) 1901–1905.
- [13] E. Shi, L. Zhang, Z. Li, P. Li, Y. Shang, Y. Jia, J. Wei, K. Wang, H. Zhu, D. Wu, S. Zhang, A. Cao, *Sci. Rep.* 2 (2012) 884.
- [14] W. Xu, S. Wu, X. Li, M. Zou, L. Yang, Z. Zhang, J. Wei, S. Hu, Y. Li, A. Cao, *Adv. Energy Mater.* 6 (2016) 1600095.
- [15] F.J. Wang, D. Kozawa, Y. Miyauchi, K. Hiraoka, S. Mouri, Y. Ohno, K. Matsuda, *Nat. Commun.* 6 (2015) 6305.
- [16] S. Del Gobbo, P. Castrucci, S. Fedele, L. Riele, A. Convertino, M. Morbidoni, F. De Nicola, M. Scarselli, L. Camilli, M. De Crescenzi, *J. Mater. Chem. C* 1 (2013) 6752–6758.
- [17] J.M. Harris, M.R. Semler, S. May, J.A. Fagan, E.K. Hobbie, *J. Phys. Chem. C* 119 (2015) 10295–10303.
- [18] S. Avasthi, S. Lee, Y.-L. Loo, J.C. Sturm, *Adv. Mater.* 23 (2011) 5762–5766.
- [19] S. Jackle, M. Mattiza, M. Liebhaber, G. Bronstrup, M. Rommel, K. Lips, S. Christiansen, *Sci. Rep.* 5 (2015) 13008.
- [20] M.J. Sailor, E.J. Ginsburg, C.B. Gorman, A. Kumar, R.H. Grubbs, N.S. Lewis, *Science* 249 (1990) 1146–1149.
- [21] X. Shen, B. Sun, D. Liu, S.-T. Lee, *J. Am. Chem. Soc.* 133 (2011) 19408–19415.
- [22] Y.F. Zhang, W. Cui, Y.W. Zhu, F.S. Zu, L.S. Liao, S.T. Lee, B.Q. Sun, *Energ. Environ. Sci.* 8 (2015) 297–302.
- [23] L. He, C. Jiang, Rusli, D. Lai, H. Wang, *Appl. Phys. Lett.* 99 (2011) 021104.
- [24] K.T. Park, H.J. Kim, M.J. Park, J.H. Jeong, J. Lee, D.G. Choi, J.H. Lee, J.H. Choi, *Sci. Rep.* 5 (2015) 12093.
- [25] S.Q. Ren, M. Bernardi, R.R. Lunt, V. Bulovic, J.C. Grossman, S. Gradecak, *Nano Lett.* 11 (2011) 5316–5321.
- [26] J.X. Wang, H. Wang, A.B. Prakoso, A.S. Togonal, L. Hong, C.Y. Jiang, *Nanoscale* 7 (2015) 4559–4565 (Rusli).
- [27] P.R. Pudasaini, F. Ruiz-Zepeda, M. Sharma, D. Elam, A. Ponce, A.A. Ayon, *ACS Appl. Mat. Inter* 5 (2013) 9620–9627.
- [28] M. Sharma, P.R. Pudasaini, F. Ruiz-Zepeda, D. Elam, A.A. Ayon, *ACS Appl. Mat. Inter* 6 (2014) 4356–4363.
- [29] T. Subramani, H.-J. Syu, C.-T. Liu, C.-C. Hsueh, S.-T. Yang, C.-F. Lin, *ACS Appl. Mat. Inter* 8 (2016) 2406–2415.
- [30] P. Yu, C.-Y. Tsai, J.-K. Chang, C.-C. Lai, P.-H. Chen, Y.-C. Lai, P.-T. Tsai, M.-C. Li, H.-T. Pan, Y.-Y. Huang, C.-I. Wu, Y.-L. Chueh, S.-W. Chen, C.-H. Du, S.-F. Horng, H.-F. Meng, *ACS Nano* 7 (2013) 10780–10787.
- [31] J. He, P.Q. Gao, M.D. Liao, X. Yang, Z.Q. Ying, S.Q. Zhou, J.C. Ye, Y. Cui, *ACS Nano* 9 (2015) 6522–6531.
- [32] Y. Liu, Z. Zhang, Z. Xia, J. Zhang, Y. Liu, F. Liang, Y. Li, T. Song, X. Yu, S.-t. Lee, B. Sun, *ACS Nano* 10 (2016), 2016, pp. 704–712.
- [33] S. Jeong, E.C. Garnett, S. Wang, Z. Yu, S. Fan, M.L. Brongersma, M.D. McGehee, Y. Cui, *Nano Lett.* 12 (2012) 2971–2976.
- [34] I. Khatri, Z.G. Tang, Q.M. Liu, R. Ishikawa, K. Ueno, H. Shirai, *Appl. Phys. Lett.* 102 (2013) 063508.
- [35] X.-Q. Bao, L.F. Liu, *Mater. Chem. Phys.* 149–150 (2015) 309–316.
- [36] M. Syed Abdul, N. Ahmed Muhammad, U. Han-Don, J. Sang-Won, C. Hyung Koun, K. Sang-Woo, L. Jung-Ho, *Nanotechnology* 23 (2012) 145401.
- [37] Z.M. Liang, M.Z. Su, H. Wang, Y.T. Gong, F.Y. Xie, L. Gong, H. Meng, P.Y. Liu, H.J. Chen, W.G. Xie, J. Chen, *ACS Appl. Mat. Inter* 7 (2015) 5830–5836.
- [38] D.D. Tune, B.S. Flavel, J.S. Quinton, A.V. Ellis, J.G. Shapter, *ChemSusChem* 6 (2013) 320–327.
- [39] L. Yu, D.D. Tune, C.J. Shearer, J.G. Shapter, *ChemNanoMat* 1 (2015) 115–121.
- [40] W. Ma, L. Song, R. Yang, T. Zhang, Y. Zhao, L. Sun, Y. Ren, D. Liu, L. Liu, J. Shen, Z. Zhang, Y. Xiang, W. Zhou, S. Xie, *Nano Lett.* 7 (2007) 2307–2311.
- [41] P. Luan, N. Zhang, W. Zhou, Z. Niu, Q. Zhang, L. Cai, X. Zhang, F. Yang, Q. Fan,

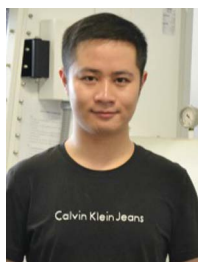
- W. Zhou, Z. Xiao, X. Gu, H. Chen, K. Li, S. Xiao, Y. Wang, H. Liu, S. Xie, *Adv. Funct. Mater.* 26 (2016) 8178–8184.
- [42] J. Sheng, K. Fan, D. Wang, C. Han, J. Fang, P. Gao, J. Ye, *ACS Appl. Mat. Inter* 6 (2014) 16027–16034.
- [44] Y. Jia, P.X. Li, X.C. Gui, J.Q. Wei, K.L. Wang, H.W. Zhu, D.H. Wu, L.H. Zhang, A.Y. Cao, Y. Xu, *Appl. Phys. Lett.* 98 (2011) 133115.
- [45] Y.H. Kim, C. Sachse, M.L. Machala, C. May, L. Mueller-Meskamp, K. Leo, *Adv. Funct. Mater.* 21 (2011) 1076–1081.
- [46] K. Fehse, R. Meerheim, K. Walzer, K. Leo, W. Lövenich, A. Elschner, *Appl. Phys. Lett.* 93 (2008) 083303.
- [47] D. Zhang, K. Ryu, X. Liu, E. Polikarpov, J. Ly, M.E. Tompson, C. Zhou, *Nano Lett.* 6 (2006) 1880–1886.
- [48] S.S. Hegedus, W.N. Shafarman, *Prog. Photovolt.* 12 (2004) 155–176.
- [49] W.B. Zhou, Q.X. Fan, Q. Zhang, K.W. Li, L. Cai, X.G. Gu, F. Yang, N. Zhang, Z.J. Xiao, H.L. Chen, S.Q. Xiao, Y.C. Wang, H.P. Liu, W.Y. Zhou, S.S. Xie, *Small* 12 (2016) 3407–3414.
- [50] A. Kaskela, A.G. Nasibulin, M.Y. Timmermans, B. Aitchison, A. Papadimitratos, Y. Tian, Z. Zhu, H. Jiang, D.P. Brown, A. Zakhidov, E.I. Kauppinen, *Nano Lett.* 10 (2010) 4349–4355.
- [51] A.S. Erickson, A. Zohar, D. Cahen, *Adv. Energy Mater.* 4 (2014) 1301724.
- [52] K.K.N.S.M. Sze, *Physics of Semiconductor Devices*, John Wiley & Sons, Inc, 2006.
- [53] Y.-J. Lin, C.-L. Tsai, Y.-C. Su, D.-S. Liu, *Appl. Phys. Lett.* 100 (2012) 253302.
- [54] M.S. Fuhrer, B.M. Kim, T. Durkop, T. Brintlinger, *Nano Lett.* 2 (2002) 755–7759.
- [55] E.S. Snow, P.M. Campbell, M.G. Ancona, J.P. Novak, *Appl. Phys. Lett.* 86 (2005) 033105.



Dr. Qingxia Fan received her B.S. degree (2011) in material physics from University of Science and Technology, Beijing. She obtained her Ph.D. degree from Institute of Physics, Chinese Academy of Sciences in 2017. Her research is mainly focused on the synthesis of carbon nanotubes and their application in solar cells.



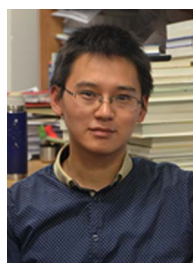
Dr. Qiang Zhang earned his B.S. degree in physics from Ocean University of China in 2010. He obtained his MSc degree (2013) in Materials Engineering and Ph.D. degree in Condensed Matter Physics from Institute of Physics, Chinese Academy of Sciences. He has joined the Department of Applied Physics, Aalto University as a postdoctoral research fellow since 2016. His current research involves the direct fabrication of CNT films as transparent conductive materials by floating catalyst CVD method and investigation of controlled synthesis of Single-Walled Carbon Nanotubes.



Dr. Wenbin Zhou received his B.S. degree (2011) in material physics from University of Science and Technology, Beijing. He obtained his Ph.D. degree from Institute of Physics, Chinese Academy of Sciences in 2016. His research is mainly focused on the synthesis of macroscopic carbon nanotubes and their thermoelectric properties as well as related applications. Currently, he is an assistant researcher in Institute of Engineering Thermophysics, Chinese Academy of Sciences.



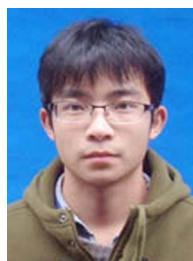
Xiaogang Xia earned his B.S. degree from Zhengzhou University in 2014. Currently, he is a Ph.D. candidate in condensed matter physics at Institute of Physics, Chinese Academy of Sciences. His research now is mainly focused on the synthesis and applications of carbon nanotubes.



Feng Yang received his B.S. degree from Department of Physics, Zhejiang Sci-Tech University in 2011. He is currently a Ph.D. candidate in the Institute of Physics, Chinese Academy of Sciences. His current research is the electronics, photonics and new type devices based on aligned single-walled carbon nanotubes and other low dimensional semiconductors by spectroscopy and Micro-nanofabrication techniques.



Dr. Nan Zhang earned his B.S. degree from the Ocean University of China (2011) and his Ph.D. degree from the Chinese Academy of Sciences (2016). Currently, he is a research fellow in Institute of Physics, Chinese Academy of Sciences. His current research interest is mainly focused on the synthesis and characterization of nano-materials as well as their applications in flexible/epidermal electronics and energy storage devices.



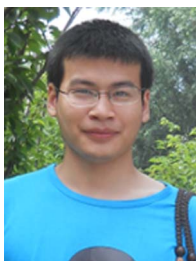
Shiqi Xiao earned his B.S. degree from Wuhan University in 2013. He is a Ph.D. candidate in Institute of Physics, Chinese Academy of Sciences. His current research is mainly focused on synthesis and application of graphene based hybrid films.



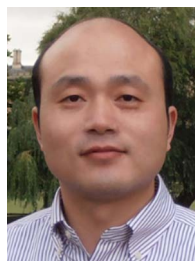
Kewei Li received his B.S. degree from Shandong University, China (2009), and his M.Eng from the Chinese Academy of Sciences (2016). His research interest includes the synthesis and application of nanomaterial-based film and fiber.



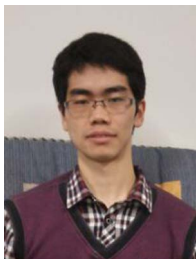
Xiaogang Gu received his B.S. degree (2012) in material physics from University of Science and Technology, Beijing. He is a Ph.D. candidate in Institute of Physics, Chinese Academy of Sciences. His research is focused on the synthesis of carbon nano materials and their application in actuators & sensors.



Zhuojian Xiao received his B.S. degree in material physics from the University of Science and Technology, Beijing in 2012. He gained his Master degree (2015) at Institute of Physics, Chinese Academy of Sciences and is a Ph.D. candidate in the same group currently. His research now is mainly focused on synthesis and application of nanomaterials based on graphene.



Prof. Huaping Liu received his Ph.D. degree from Beijing Normal University in 2006. After that, he worked as a postdoctoral fellow in the Abdus Salam International Centre for Theoretical Physics (ICTP) and Elettra Sincrotrone (Trieste, Italy), Tokyo University of Science and the National Institute of Advanced Industrial Science and Technology (AIST), Japan. At the beginning of 2013, he joined Institute of Physics, Chinese Academy of Sciences by the Recruitment Program of Global Youth Experts of China. His current research mainly includes the synthesis, separation, optoelectronic properties of carbon nanotubes and their application in flexible devices.



Huiliang Chen earned his B.S. degree from Zhengzhou University in 2013. Currently, he is a Ph.D. candidate in institute of physics, Chinese Academy of Sciences. His research now is mainly focused on energy storage materials based on carbon materials.



Prof. Weiya Zhou received her Ph.D. degree from Jilin University in 1990. After a postdoctoral research at the university of Groningen (the Netherlands), she joined the institute of physics, Chinese Academy of Sciences. She has been engaged a long time in the investigation of carbon nanotubes or the relevant nanomaterials and their characterization as well as their physical properties and possible applications.



Dr. Yanchun Wang received his Ph.D. degree from the institute of physics, Chinese Academy of Sciences in 2008. He has been worked as a postdoctoral research fellow at Hongkong University from 2009 to 2011.



Prof. Sishen Xie is a physicist and an academian at the Chinese Academy of Sciences (CAS) and a fellow of the Third World Academy of Sciences. He graduated in physics from Peking University in 1965 and received his Ph.D. degree in 1983 from the Institute of Physics at CAS. His research interests are mainly in solid-state and materials physics, including high-T_c superconductivity of oxides, phase diagrams and relations of inorganic systems, fullerenes, and nanomaterials.